

Evidence of cation vacancy induced room temperature ferromagnetism in Li-N codoped ZnO thin films

B. Y. Zhang, B. Yao, Y. F. Li, A. M. Liu, Z. Z. Zhang et al.

Citation: *Appl. Phys. Lett.* **99**, 182503 (2011); doi: 10.1063/1.3657412

View online: <http://dx.doi.org/10.1063/1.3657412>

View Table of Contents: <http://apl.aip.org/resource/1/APPLAB/v99/i18>

Published by the [American Institute of Physics](#).

Related Articles

Magnetic domain pattern asymmetry in (Ga, Mn)As/(Ga, In)As with in-plane anisotropy

J. Appl. Phys. **111**, 083908 (2012)

Magnetoresistive effects in perpendicularly magnetized Tb-Co alloy based thin films and spin valves

J. Appl. Phys. **111**, 083904 (2012)

Epitaxial ferromagnetic nanoislands of cubic GdN in hexagonal GaN

Appl. Phys. Lett. **100**, 152111 (2012)

Effect of silver addition on structural, electrical and magnetic properties of Fe₃O₄ thin films prepared by pulsed laser deposition

J. Appl. Phys. **111**, 073907 (2012)

Microstructure and magnetization reversal of L1₀-FePt/[Co/Pt]_N exchange coupled composite films

Appl. Phys. Lett. **100**, 142406 (2012)

Additional information on *Appl. Phys. Lett.*

Journal Homepage: <http://apl.aip.org/>

Journal Information: http://apl.aip.org/about/about_the_journal

Top downloads: http://apl.aip.org/features/most_downloaded

Information for Authors: <http://apl.aip.org/authors>

ADVERTISEMENT

<p>INSTRUMENTS FOR ADVANCED SCIENCE</p> 			
Gas Analysis dynamic measurement of reaction gas streams catalysis and thermal analysis molecular beam studies dissolved species probes fermentation, environmental and ecological studies	Surface Science UHV TPD SIMS end point detection in ion beam etch elemental imaging - surface mapping	Plasma Diagnostics plasma source characterisation etch and deposition process reaction kinetic studies analysis of neutral and radical species	Vacuum Analysis partial pressure measurement and control of process gases reactive sputter process control vacuum diagnostics vacuum coating process monitoring
<p>contact Hiden Analytical for further details: info@hiden.co.uk www.HidenAnalytical.com CLICK TO VIEW OUR PRODUCT CATALOGUE</p>			
			

Evidence of cation vacancy induced room temperature ferromagnetism in Li-N codoped ZnO thin films

B. Y. Zhang,^{1,2} B. Yao,^{1,3,a)} Y. F. Li,^{3,4} A. M. Liu,² Z. Z. Zhang,¹ B. H. Li,¹ G. Z. Xing,^{3,4} T. Wu,⁴ X. B. Qin,⁵ D. X. Zhao,¹ C. X. Shan,¹ and D. Z. Shen¹

¹Key Laboratory of Excited State Process, Changchun Institute of Optics, Fine Mechanics and Physics, Chinese Academy of Science, Changchun 130033, People's Republic of China

²School of Physics and Optoelectronic Technology, Dalian University of Technology, Dalian 116023, People's Republic of China

³State Key Laboratory of Superhard Material, Department of Physics, Jilin University, Changchun 130023, People's Republic of China

⁴Division of Physics and Applied Physics, School of Physical and Mathematical Sciences, Nanyang Technological University, Singapore 637371, Singapore

⁵Key Laboratory of Nuclear Analysis Techniques, Institute of High Energy Physics, Chinese Academy of Sciences, Beijing 100049, People's Republic of China

(Received 10 August 2011; accepted 9 October 2011; published online 31 October 2011)

Room temperature ferromagnetism (RTFM) was observed in Li-N codoped ZnO thin films [ZnO:(Li, N)] fabricated by plasma-assisted molecular beam epitaxy, and p-type ZnO:(Li, N) shows the strongest RTFM. Positron annihilation spectroscopy and low temperature photoluminescence measurements indicate that the RTFM in ZnO:(Li, N) is attributed to the defect complex related to V_{Zn} , such as V_{Zn} and $Li_i-N_O-V_{Zn}$ complex, well supported by first-principles calculations. The incorporation of N_O can stabilize and enhance the RTFM of ZnO:(Li, N) by combining with Li_i to form Li_i-N_O complex, which restrains the compensation of Li_i for V_{Zn} and makes the ZnO:(Li, N) conduct in p-type. © 2011 American Institute of Physics. [doi:10.1063/1.3657412]

Dilute magnetic semiconductors (DMSs) have attracted much interest due to their favorable magnetic, magneto-optical, and magneto-electrical properties for application of spin-dependent electronic devices.¹ In the past decade, ZnO has been extensively investigated as a candidate DMS host material because it was predicted to have room temperature ferromagnetism (RTFM) as doped by transition metals (TMs), such as Mn and Co, etc.² However, the origin of the RTFM is still argued. Some researchers attribute the RTFM to the magnetic atoms incorporating into ZnO, but others assign the RTFM to the uncontrolled Mn or Co clusters or their secondary phases.³ Recently, some research groups found that nonmagnetic ion doped ZnO also exhibit ferromagnetism, namely, so called “*d*” FM.⁴ However, ferromagnetic properties of ZnO thin films doped by nonmagnetic ion are strongly dependent on growth condition. Some researchers believed that the correlation between FM and growth conditions suggest that defects may play an important role in the observed magnetic behaviors of ZnO.⁵ Although several experimental and theoretical investigations have been carried out, the mechanism behind the enhancement of FM by doping nonmagnetic ion is still conflict.

Recently, many reports indicated that an additional hole doping is essential to stabilized the ferromagnetic ground state in DMS.⁶ Therefore, choosing appropriate acceptor dopant is proven to be a proper method to enhance the RTFM. As the best candidates for achieving p-type ZnO, Li and N have attracted our attention due to the matching of their atomic radius with Zn and O and shallow acceptor levels. Many studies have been carried out to clarify the origin of the FM for Li doped ZnO thin films.⁷ Especially, Yi

*et al.*⁸ have achieved the RTFM by doping Li and proposed that the origin of RTFM is due to the V_{Zn} induced by Li doping in ZnO. However, one ultimate challenge is the amphoteric nature of Li, where Li acts as a donor on an interstitial site (Li_i), but an acceptor on a substitutional site (Li_{Zn}), leading to self-compensation. Based on the density functional theory, Wardle *et al.*⁹ have predicted the existence of the neutral Li_i-Li_{Zn} complex. The compensation between Li_{Zn} and Li_i decreases the hole concentration of ZnO, resulting in decreasing of RTFM. Therefore, in our previous work, the Li and N codoped method is proposed to solve the self-compensation problem.¹⁰ The introduction of N_O is expected to enhance the RTFM by formation of Li_i-N_O complex, which depresses the compensation of Li_i for Li_{Zn} and V_{Zn} , and makes V_{Zn} concentration increase and ZnO conduct in p-type.

In this study, in order to identify the origin of the RTFM of Li-N codoped ZnO [ZnO:(Li, N)], a series of ZnO:(Li, N) with different Li doping concentration were fabricated on c-sapphire substrates by plasma-assisted molecular beam epitaxy (P-MBE) using high pure metal Zn, Li, and NO as metal and gas source, respectively. Temperature-dependent photoluminescence (TDPL) was measured using the He-Cd laser line of 325 nm as the excitation source. The compositions of ZnO:(Li, N) thin films were detected by time-of-flight secondary ion mass spectrometry (TOF-SIMS) (TOF-SIMS IV instrument from IONTOF GmbH). Electrical properties were characterized with the Van der Pauw configuration in a Hall effect measurement system. Magnetization measurements were carried out by using a high sensitive superconducting quantum interference devices magnetometer (SQUID, Quantum Design). The thickness of the ZnO films was determined by field-emission scanning electronic microscope (FESEM).

^{a)}Electronic mail: binyao@jlu.edu.cn.

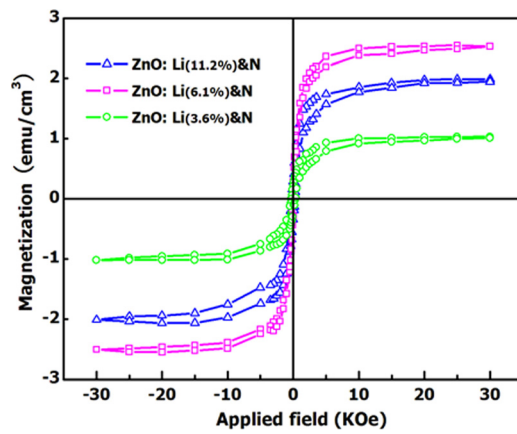


FIG. 1. (Color online) Room temperature magnetic hysteresis loops of ZnO:(Li, N) thin films with various Li doping concentration.

The volume of the films was estimated to be 1×10^{-5} , 1.26×10^{-5} , and $4.25 \times 10^{-6} \text{ cm}^3$ for Li doping concentration of 3.6%, 6.1%, and 11.2%, respectively. Furthermore, the volume and magnetization measurements were carried out repeatedly and the average values were treated as final results to reduce measurement error.¹¹ The diamagnetic background of the sapphire substrates was carefully calibrated and subtracted from the raw data. Positron annihilation experiments (PAS) were performed to identify the cation vacancy at room temperature with a monoenergetic positron beam. Positrons were implanted at energies from 0 to 20 keV.

Figure 1 shows the M-H loops measured at room temperature for the ZnO:(Li, N) thin films with Li doping concentration of 3.6%, 6.1%, and 11.2%. With the increase of Li doping concentration to 3.6%, the ZnO:(Li, N) thin films shows FM properties and n-type conductivity, and the saturation magnetization (M_s) increases to 1.1 emu/cm^3 . When the Li doping concentration reaches to 6.1%, the ZnO:(Li, N) transforms from n-type to p-type with the hole concentration of $8.2 \times 10^{16} \text{ cm}^{-3}$ and a mobility of $1.4 \text{ cm}^2/\text{V s}$, and the M_s increases significantly to 2.5 emu/cm^3 . With further increase of Li doping concentration to 11.2%, the sample becomes insulating, and the M_s decreases to 1.6 emu/cm^3 .

As expected, the undoped ZnO shows n-type conduction. With the increasing of Li doping concentration, resistivity and carrier concentration of ZnO:(Li, N) thin films increase and decrease, respectively. As the Li concentration reaches to 6.1%, the ZnO:(Li, N) transforms from n-type to p-type and has kept stable p-type conductivity. The origin of p-type conductivity is attributed to Li_{Zn} and V_{Zn} .^{10,12} More details of the electrical properties of undoped ZnO and ZnO:(Li, N) can be found in our previous works.¹⁰

To explore the origin of the RTFM, SIMS, and TDPL measurements were performed, as shown in Fig. 2. Figures 2(a) and 2(b) show the depth profile of the main elements in ZnO:(Li, N) thin films with Li doping concentration of 6.1% and 11.2%, respectively. As expected, the concentrations of Zn and O were constants across the ZnO:(Li, N). Moreover, the measurements show that Li and N are incorporated into ZnO and uniformly distributed throughout the ZnO:(Li, N) thin films. Figures 2(c) and 2(d) show the 80 K PL spectra of undoped ZnO and ZnO:(Li, N) with Li doping concentration of 11.2%, respectively. For the undoped sample, there reveals

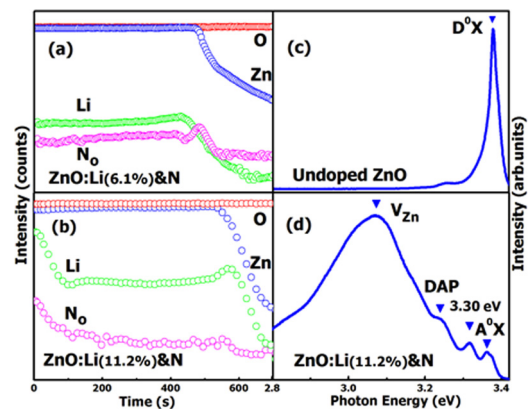


FIG. 2. (Color online) The TOF-SIMS depth profile of ZnO:(Li, N) thin films with Li concentration of (a) 6.1% and (b) 11.2%, respectively, as well as the 80 K PL spectra of (c) undoped ZnO and (d) ZnO:(Li, N) thin films with Li concentration of 11.2%.

a strong ultraviolet emission located at 3.36 eV , which is assigned to the neutral-donor bound excitons (D^0X).¹³ For the sample with Li concentration of 11.2%, there exist four peaks in the blue-ultraviolet range, located at 3.34 , 3.30 , 3.22 , and 3.06 eV , respectively, which are attributed to neutral-acceptor bound excitons (A^0X), stacking faults, donor-acceptor pair transition (DAP), and the electron transition from conduction-band minimum (CBM) to V_{Zn} level, respectively.^{13–15} The 3.06 eV peak is dominant, hence, we speculate a large amount of V_{Zn} in the ZnO:(Li, N) thin films.

To verify the scenario, positron annihilation spectroscopy (PAS) measurements were performed to detect cation vacancies. It is well known that PAS is very sensitive to negatively charged and neutral vacancy-type defects and has been proved to be a powerful tool to investigate vacancy defects in semiconductor.¹⁶ With the help of PAS, the vacancy defects can be identified and their concentrations are determined. Figure 3 shows the plots of the S parameter as a function of positron implantation energy for the undoped ZnO and ZnO:(Li, N) with Li doping concentration of 11.2%. The inset shows the plots of the W values as a function of S value for the both samples. It can be seen from the inset that the S and W values lie on a straight line, which means that the two samples contain the same vacancy defects.¹⁷ It is well known that V_{Zn} are dominant acceptors in undoped ZnO. Therefore, based on the above discussion, V_{Zn} related defects are the main defect trapping positrons inside the films. Based on change of the S shown in Fig. 3, the plots can be divided into three parts. In the part I of energy range of 0 to 2 keV , the S decreases sharply with increasing energy and both plots overlap, which is due to the positron annihilations and formation of positronium atoms at the surface of the samples.¹⁸ The plots in the part II of energy range between 2 and 8 keV can be regarded as the characteristic of the two samples. In the part II, the S parameter of the ZnO:(Li, N) shows a distinct increase, in comparison with undoped ZnO, implying that the amount of V_{Zn} increases with the increasing of Li doping concentration. While in the part III of energy range of $8\text{--}20 \text{ keV}$, positrons annihilate mainly in the sapphire substrate, leading to overlapping of the two plots.

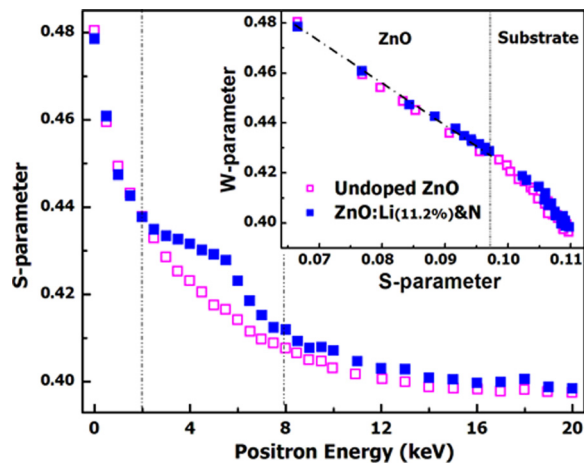


FIG. 3. (Color online) S values as a function of incident positron energy (E , keV) for the samples: undoped ZnO and ZnO:(Li, N) with Li concentration of 11.2%. The inset shows the W values as a function of S value.

According to recent reports, V_{Zn} can provide magnetic moment in both ZnO and ZnMgO.^{5,19} In order to well understand the origin of FM, the electronic structure and density of states of V_{Zn} and Li_{Zn} and defect complexes of Li_i-N_O and Li_i-V_{Zn} in ZnO:(Li, N) were calculated by using first-principles based on density-functional theory. It is found that Li_{Zn} , Li_i-N_O , and Li_i-V_{Zn} complexes are not capable to contribute to magnetic moment. However, a single V_{Zn} favors a spin polarized state and each V_{Zn} carries a magnetic moment of $1.82 \mu_B$. In addition, some other types of complex defects are also taken into consideration, such as $Li_i-Li_{Zn}-V_{Zn}$ and $Li_i-N_O-V_{Zn}$. It is noted that the $Li_i-Li_{Zn}-V_{Zn}$ complex does not induce magnetic moment, but the $Li_i-N_O-V_{Zn}$ complex contributes a magnetic moment of $1.46 \mu_B$. Furthermore, we calculated the formation energy of $Li_i-Li_{Zn}-V_{Zn}$ and $Li_i-N_O-V_{Zn}$ complexes related to oxygen chemical potential. It is found that the formation energy of $Li_i-N_O-V_{Zn}$ complex is lower than that of $Li_i-Li_{Zn}-V_{Zn}$ complex, which means $Li_i-N_O-V_{Zn}$ complex forms more favorably than $Li_i-Li_{Zn}-V_{Zn}$ complex in ZnO:(Li, N). Since $Li_i-Li_{Zn}-V_{Zn}$ complex has lower formation energy than V_{Zn} throughout the entire range of oxygen chemical potential, it is indicated that an amount of $Li_i-N_O-V_{Zn}$ complexes exists in ZnO:(Li, N) and contributes to FM.⁸ Base on the experimental and theoretical results mentioned above, it is deduced that the origin of FM of ZnO:(Li, N) thin films is related to V_{Zn} and $Li_i-N_O-V_{Zn}$ complex.

Recently, several reports suggested that N_O results in magnetism due to the unpaired 2p electron of N and O atoms in N doped ZnO.²⁰ However, N_O cannot contribute to magnetism of the ZnO:(Li, N), since it easily combines with Li_i to form non-magnetic Li_i-N_O complex.¹⁰ Although the formation of the Li_i-N_O annihilates the N_O magnetism, it makes more V_{Zn} contribute magnetism by depressing the compensation of Li_i for V_{Zn} . Therefore, the incorporation of N can enhance and stabilize the FM of ZnO:(Li, N). The recent investigation on Li monodoped ZnO indicated that more V_{Zn} are induced in ZnO with increasing Li doping concentration, leading to the increment of Ms.⁸ However, in the present work, the Ms of ZnO:(Li, N) increases initially and then decreases as Li concentration increases in the range of 0%–11.2%. It can be explained as follows: When Li doping

concentration is in a low range, a small amount of V_{Zn} is induced in ZnO:(Li, N) and possible compensation of Li_i for V_{Zn} is depressed by formation of Li_i-N_O complex, leading to weak FM. When Li doping concentration increases continuously, more V_{Zn} are generated, resulting in the increase of FM. With further increasing of Li concentration, some Li_i may not combine with N_O to form Li_i-N_O complex due to the limited solubility of N_O in ZnO. The excessive Li_i will compensate for V_{Zn} by formation of non-magnetic Li_i-V_{Zn} complex and make the Ms decrease.

In summary, RTFM was observed in ZnO:(Li, N) thin films grown on c-sapphire by P-MBE. The Ms of ZnO:(Li, N) increases with increasing Li doping concentration in the range of 0%–6.1%, but decreases from 6.1% to 11.2%, and p-type ZnO:(Li, N) shows the strongest RTFM. The RTFM of ZnO:(Li, N) is attributed to V_{Zn} and $Li_i-N_O-V_{Zn}$ complex. The incorporation of N_O can stabilize and enhance the RTFM by formation of the Li_i-N_O complex, which yields more V_{Zn} by restraining compensation of Li_i for V_{Zn} .

This work is supported by National Basic Research Program of China (973 Program) under Grant No. 2011CB302005, the National Natural Science Foundation of China under Grant Nos. 60776011, 10874178, 11074248, and 60806002, Natural Science Foundation of Jilin province under Grant No. 201115013, and Swedish Research Council.

- ¹J. Pearton, W. H. Heo, M. Ivill, D. P. Norton, and T. Steiner, *Semicond. Sci. Technol.* **19**, R59 (2004).
- ²T. Dietl, H. Ohno, F. Matsukura, J. Cibert, and D. Ferrand, *Science* **287**, 1019 (2000).
- ³S. M. Heald, T. Kaspar, T. Droubay, V. Shutthanandan, S. Chambers, A. Mokhtari, A. J. Behan, H. J. Blythe, J. R. Neal, A. M. Fox, and G. A. Gehring, *Phys. Rev. B* **79**, 075202 (2009).
- ⁴T. S. Herg, S. P. Lau, L. Wang, B. C. Zhao, S. F. Yu, M. Tanemura, A. Akaike, and K. S. Teng, *Appl. Phys. Lett.* **95**, 012505 (2009).
- ⁵G. Xing, D. Wang, J. Yi, L. Yang, M. Gao, M. He, J. Yang, J. Ding, T. C. Sum, and T. Wu, *Appl. Phys. Lett.* **96**, 112511 (2010).
- ⁶I. S. Elfimov, A. Rusydi, S. I. Csiszar, Z. Hu, H. H. Hsieh, H. J. Lin, C. T. Chen, R. Liang, and G. A. Sawatzky, *Phys. Rev. Lett.* **98**, 137202 (2007).
- ⁷S. Chawla, K. Jayanthi, and R. K. Kotnala, *Phys. Rev. B* **79**, 125204 (2009).
- ⁸J. B. Yi, C. C. Lim, G. Z. Xing, H. M. Fan, L. H. Van, S. L. Huang, K. S. Yang, X. L. Huang, X. B. Qin, B. Y. Wang, T. Wu, L. Wang, H. T. Zhang, X. Y. Gao, T. Liu, A. T. S. Wee, Y. P. Feng, and J. Ding, *Phys. Rev. Lett.* **104**, 137201 (2010).
- ⁹M. G. Wardle, J. P. Goss, and P. R. Briddon, *Phys. Rev. B* **71**, 155205 (2005).
- ¹⁰B. Y. Zhang, B. Yao, Y. F. Li, Z. Z. Zhang, B. H. Li, C. X. Shan, D. X. Zhao, and D. Z. Shen, *Appl. Phys. Lett.* **97**, 222101 (2010).
- ¹¹M. A. Garcia, E. F. Pinel, J. de la Venta, A. Quesada, V. Bouzas, J. F. Fernández, J. J. Romero, M. S. M. González, and J. L. Costa-Krämer, *J. Appl. Phys.* **105**, 013925 (2009).
- ¹²T. T. Zhao, T. Yang, B. Yao, C. X. Cong, Y. R. Sui, G. Z. Xing, Y. Sun, S. C. Su, H. Zhu, and D. Z. Shen, *Thin Solid Films* **518**, 3289 (2010).
- ¹³D. C. Look, D. C. Reynolds, C. W. Litton, R. L. Jones, D. B. Eason, and G. Cantwell, *Appl. Phys. Lett.* **81**, 1830 (2002).
- ¹⁴B. X. Lin, Z. X. Fu, and Y. B. Jia, *Appl. Phys. Lett.* **79**, 943 (2001).
- ¹⁵M. Schirra, R. Schneider, A. Reiser, G. M. Prinz, M. Feneberg, J. Biskuppek, U. Kaiser, C. E. Krill, K. Thonke, and R. Sauer, *Phys. Rev. B* **77**, 125215 (2008).
- ¹⁶F. Tuomisto, V. Ranki, D. C. Look, and G. C. Farlow, *Phys. Rev. B* **76**, 165207 (2007).
- ¹⁷L. Liskay, C. Corbel, and L. Baroux, *Appl. Phys. Lett.* **64**, 1380 (1994).
- ¹⁸A. L. Yang, H. P. Song, D. C. Liang, H. Y. Wei, X. L. Liu, P. Jin, X. B. Qin, S. Y. Yang, Q. S. Zhu, and Z. G. Wang, *Appl. Phys. Lett.* **96**, 151904 (2010).
- ¹⁹Y. F. Li, R. Deng, B. Yao, G. Z. Xing, D. D. Wang, and T. Wu, *Appl. Phys. Lett.* **97**, 102506 (2010).
- ²⁰D. Q. Fang, A. L. Rosa, R. Q. Zhang, and Th. Frauenheim, *J. Phys. Chem. C* **114**, 5760 (2010).